BULLETIN OF THE CHEMICAL SOCIETY OF JAPAN VOL. 43 2690—2702 (1970)

Photoemission from Organic Crystal in Vacuum Ultraviolet Region. IV

Masakatsu KOCHI,*1 Yoshiya HARADA, Tomohiko HIROOKA and Hiroo INOKUCHI

The Institute for Solid State Physics, The University of Tokyo, Roppongi, Tokyo

(Received February 7, 1970)

The quantum yield and the energy distribution of photoelectrons were measured for organic crystals in the vacuum ultraviolet region. A model was presented for the photoemission from organic crystals with a narrow valence band, and a semiempirical power law was derived for the yield near the threshold. The ionization potentials found from the spectral distribution of the quantum yield using this model were as follows: anthracene—5.68 eV, naphthacene—5.43, pentacene—5.04, perylene—5.33, indanthrone—5.17, and tetrathionaphthacene—4.42. The effect of electrons which escape after one inelastic scattering was observed. It was shown how the contribution of once-scattered electrons can be separated in the energy distribution. The threshold for "pair production" was estimated to be nearly equal to the band gap for perylene and a little higher than the band gap for quaterrylene. The fine structures observed both in the yield spectra and in the energy distribution can be accounted for by assuming the existence of additional valence bands.

Photoemission from solids is considered to be a three-step process: first, electrons are optically excited into high energy states; second, the excited electrons move to the surface of solids, with or without inelastic scattering, and third, they escape over the surface barrier into a vacuum. We define the first process as an optical excitation process, and the latter two as transport processes. In order to study these processes in solids, measurements of the spectral distribution of the photoelectric yield and the energy distribution of photoemitted electrons at individual photon energies can be used. As a result, the analysis of photoemission from solids gives us information on the electronic states and the transport phenomena in the solids. Recently, ultraviolet photoemission has received increasing attention as an experimental method of probing the electronic structure in solid.[1-4]

Although the external photoelectric emission from organic cystals has been measured by several workers,[5-10] there have been no systematic studies about the total process mentioned above.

In this paper, the photoemission both at photon energy near the threshold and well above the threshold is investigated. The well-known fact that an intermolecular interaction in organic crystal is very weak as compared with that in metal or inorganic semiconductor is taken into account by considering the intramolecular vibrations. With regard to the transport process, inelastic scattering between electrons and the tunneling effect over the surface barrier is emphasized. By these means, general results are obtained which allow a considerably detailed interpretation of the photoemissive characters of the organic crystals.

Method of Analysis

1.1 A Model for the Photoemission from Organic Crystals. In the study of photoelectric phenomena in solids, the photoemission from metals has been investigated most extensively, and the work functions of metals have been obtained by using a method developed by Fowler.[11]

The photoemission from inorganic semiconductors is treated on the assumption of "density of state" considerations. Precise studies[12] of weak

*1 Present address: The Institute of Space and Aeronautical Science, The University of Tokyo, Komaba, Tokyo.

1) C. N. Berglund and W. E. Spicer, *Phys. Rev.*, **136**, A 1030 (1964).
2) A. J. Blodgett, Jr., and W. E. Spicer, *ibid.*, **146**, 390 (1966).
3) T. M. Donovan and W. E. Spicer, *Phys. Rev. Lett.*, **21**, 1572 (1968).
4) D. E. Eastman, *Phys. Rev.*, **40**, 1387 (1969).
5) L. E. Lyons and G. C. Morris, *J. Chem. Soc.*, **1960**, 5192.
6) A. Terenin and F. Vilessov, *Doklady Akad. Nauk, SSSR*, **134**, 71 (1960).
7) R. C. Nelson, *J. Opt. Soc. Amer.*, **51**, 1186 (1961).
8) D. R. Kearns and M. Calvin, *J. Chem. Phys.*, **34**, 2026 (1961).
9) Y. Harada and H. Inokuchi, This Bulletin **39**, 1443 (1966).
10) M. Kochi, Y. Harada and H. Inokuchi, *ibid.*, **40**, 531 (1967).
11) R. H. Fowler, *Phys. Rev.*, **38**, 45 (1931).
12) G. W. Gobelli and F. G. Allen, *ibid.*, **127**, 141 (1962).

photoelectric emission from silicon metal near the threshold on atomically-clean surfaces reveal direct and indirect thresholds. The plot of the quantum yield against the photon energy is linear when photoelectrons are generated by optical direct transition in the bulk. An indirect transition results in the cube-root of the quantum yield becoming proportional to the photon energy. These results are in agreement with Kane's theory.[13] Kane's power laws near the threshold mainly depend on the shape of the upper edge of the valence band. Therefore, his formula can not be applied to organic crystals with narrow valence bands.

Therefore, we wish now to propose a simple model for interpreting the general results of the photoemission from organic crystals. This model uses the following assumptions:

(a) the crystal is composed of vibrating molecules, and

(b) the wavefunction of an electron part may be described by Bloch representation inside the crystal, which joins smoothly through the surface barrier to a free electron state of equal energy.

Molecular vibrations in aromatic molecules typically have energies of approximately 0.4 eV (corresponding to C–H stretching), while the bandwidths for excess holes in molecular crystals of the naphthalene · anthracene type are very narrow—0.2 eV at the largest, and possibly smaller than that by an order of magnitude or more.[14] Thus, the effect of molecular vibrations is to split each hole band into many well-separated bands, all separated by the energy of a vibrational quantum. On the other hand, an excess electron band may not be separated by a vibrational quantum, because the ionized state with a wide electronic band is considered in the study of photoemission. Figure 1 illustrates a simplified case where there is only one vibrational frequency. A parabolic band is assumed for the conduction band. The energy difference, Δ, between the vacuum level and the bottom of the band will act as a surface barrier for slow photoelectrons. The valence bands are considered to be almost flat against the change in the k vector. The energy states which should exist below the conduction band for organic crystals are omitted in Fig. 1 for the sake of simplicity.

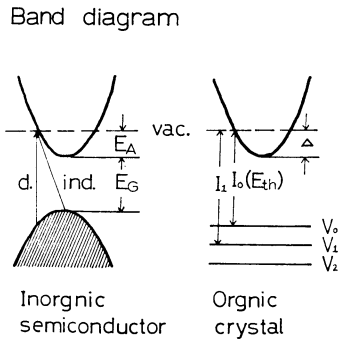

Fig. 1. Band diagram in photoemission from organic crystals including the vibronic bands. associated with hole bands.
The pure hold band is labeled V_0. Vibrationally excited bands are lebeled V_1, V_2, and so on.
(Band diagram for inorganic semiconductors is illustrated for reference; d. and ind. correspond to direct and indirect threshold, respectively.)

Assuming that no vibrational states are excited in the initial ground state, the electronic transition which puts a hole into V_0 requires only electronic excitation. The photon energy required for this pure electronic transition corresponds to the photoelectric threshold energy, E_{th}. It is denoted as I_0 in Fig. 1. Since the electronic transition which puts a hole into V_1 requires simultaneous electronic and vibrational excitation, it requires more energy than the excitation in V_0. For this reason, the vibrationally-excited hole bands are drawn downwards with increasing energy, as in Fig. 1.

1.2. The Form of the Spectral Distribution of the Quantum Yield near the Threshold. The quantum yield, $Y(h\nu)$, is designated by $Y(h\nu)$=number of electrons emitted/number of incident quanta. We assume that all the incident quanta are absorbed.*2 Then, using the first-order time-dependent perturbation theory, the quantum yield can be written as:

$$Y(h\nu) = \sum_i \int_0^\infty \int_{B.Z.} \delta(E_f - E_i - h\nu)|H_{if}|^2 \times \rho(E_f)D(E_f, x)I e^{-\alpha x} dx dE_f \Big/ \int_0^\infty I\alpha e^{-\alpha x} dx$$

and

$$\alpha = \sum_i \int_{B.Z.} \delta(E_f - E_i - h\nu)|H_{if}|^2 \rho(E_f) dE_f, \quad (1)$$

if all the photons of energy, $h\nu$, are absorbed in exciting electrons in the crystal. Here, I is the intensity of incident light; the absorption coefficient, $\alpha(h\nu)$, corresponds to the total absorption of the crystal at the photon energy, $h\nu$; H_{if} is the matrix element of the momentum; $\rho(E_f)$ is the state density, and $D(E_f,x)$ is the escape probability of an electron excited to a certain energy, E_f, at a certain distance, x, from the crystal surface. In Eq. (1) the state density of initial states is elimi-

13) E. O. Kane, *ibid.*, **127**, 131 (1962).

14) O. H. LeBlanc, *J. Chem. Phys.*, **40**, 2223 (1964); J. L. Katz, S. A. Rice, S. I. Choi, and J. Jortner, *ibid.*, **39**, 1683 (1963); R. Silbey, J. Jortner, S.A. Rice and M. Vala, *ibid.*, **42**, 733 (1965).

*2 This assumption was valid for the crystals several microns thick in the vacuum ultraviolet region. However, it may be necessary to take into account the optical reflectivity at the crystal surface for a more precise study.

nated because of the narrow band, the photoemissive crystal is assumed to be semiinfinite, and the integral with respect to E_f extends over the Brillouin zone (B.Z.).

The $D(E_f,x)$ term generally involves both the scattering probability and the surface transmission probability, $T(E_f)$. Near the threshold, $D(E_f,x)$ may be represented only by $T(E_f)$, because the scattering probability varies slowly near the threshold. The subsequent integration with respect to x gives the result:

$$Y(h\nu) = \frac{1}{\alpha(h\nu)} \sum_i \int_{B.Z.} \delta(E_f - E_i - h\nu) |H_{if}|^2 \times \rho(E_f) T(E_f) dE_f. \quad (1')$$

With the adiabatic approximation, H_{if} is expressed as follows;

$$H_{if} = M_{if}(R_0) \cdot \langle n|0\rangle. \quad (2)$$

where $M_{if}(R_0)$ is the matrix element of the electronic part at the equilibrium atomic distance, R_0, and where $\langle n|0\rangle$ is the "overlap integral" concerned with the vibrational part. By substituting Eq. (2) into Eq. (1'), we obtain:

$$Y(h\nu) = \frac{1}{\alpha(h\nu)} \sum_i \int_{B.Z.} \delta(E_f - E_i - h\nu) |\langle n|0\rangle|^2 \times |M_{if}|^2 T(E_f) \rho(E_f) dE_f. \quad (3)$$

In Eq. (3) we assume that $\alpha(h\nu)$, M_{if}, and $\rho(E_f)$ are slowly varying in the vicinity of the threshold, because, in the absorption spectra, no drastic change is found near the photon energy corresponding to the threshold energy of photoemission.[5] Hence, Eq. (3) may take the following form near the threshold:

$$Y(h\nu) \propto \sum_i \int_{B.Z.} \delta(E_f - E_i - h\nu) |\langle n|0\rangle|^2 T(E_f) dE_f. \quad (4)$$

The delta function in Eq. (4) gives the energy conservation relation:

$$E_f - E_i - h\nu = E + I_n - h\nu = 0 \quad (5)$$

In Eq. (5) the energy zero is taken to be a vacuum, E is the kinetic energy of a free electron, and I_n is the threshold energy corresponding to the n'th vibrational level:

$$I_n = I_0 + n\hbar\omega \quad (6)$$

I_0 corresponds to the ionization potential, I_c, of the crystal, and $\hbar\omega$ is the vibrational energy quanta, where the diversity of vibrational quanta due to many kinds of vibrational modes is neglected for the sake of simplicity. The critical escape condition:

$$E \geq 0, \quad (7)$$

can be expected from the transmission probability, $T(E)$. From Eqs. (4), (5), (6), and (7), the following relation is obtained:

$$Y(h\nu) \propto \sum_n [|\langle n|0\rangle|^2 \cdot T(E)]$$
$$0 \leq E = h\nu - I_0 - n\hbar\omega \leq h\nu - I_0. \quad (8)$$

Since it is difficult to calculate both factors, $T(E)$ and $|\langle n|0\rangle|^2$, especially for polyatomic molecular crystals, we determine their forms empirically as follows.

The Form of $T(E)$. The surface transmission probability, $T(E)$, is difficult to determine exactly, for it depends on the shape of the surface barrier. However, it is evident that $T(E)$ must be zero for $E=0$ and that it must increase at higher values of E. In a first approximation we set:

$$T(E) \begin{cases} = 0 & \text{for } E < 0 \\ \propto E^l \left(\frac{1}{2} \leq l \leq 1\right) & \text{for } E \geq 0 \end{cases} \quad (9)$$

Note that it is for slow electrons that the shape of the surface potential barrier becomes important and that $T(E)$ usually becomes nearly constant for a large value of E. $T(E)$ is one of the main factors determining the energy distribution of slow electrons and the form of the quantum yield near the threshold.

The Form of $|\langle n|0\rangle|^2$. Condon's "overlap integral," $\langle n|0\rangle$, in Eq. (8) was considered in connection with diatomic molecules by Mannenback.[15] In general, if the change of equilibrium interatomic distances through the excitation process is large, a $\langle 0|0\rangle$ factor often becomes small and the overlap integral in the $\langle n|0\rangle$ progressions will increase slowly with the increase in n. The energy distribution due to the $|\langle n|0\rangle|^2$ factor is observed as a broadened band in the energy-loss curve, because there are many kinds of vibrational modes in polyatomic molecules, each having different vibrational quanta. It will be found in the energy-loss curves that the number of slower electrons increases almost linearly with the increase in the energy-loss, that is to say, with the increase in the vibrational quantum number, n, commencing at the electron energy corresponding to the $0 \leftarrow 0$ vibrational transition, and reaching the first maximum. Therefore, as a first approximation we replace the $|\langle n|0\rangle|^2$ factor by a linear equation of n, setting $|\langle 0|0\rangle|^2 \simeq 0$.

Replacing $T(E)$ and $|\langle n|0\rangle|^2$ in Eq. (8) by $E^l (1/2 \leq l \leq 1)$ and n respectively, and integrating over n in place of the summation in Eq. (8), we obtain the following relation:

$$Y \propto (h\nu - E_{th})^m, \left(\frac{5}{2} \leq m \leq 3\right) \quad (10)$$

This semi-empirical power law for the yield near the threshold will be compared with the experimental results in Section 4.1.

1.3. The Effect of Pair-production Scattering on the Energy Distribution. "Pair-production scattering" means the process by which the primary electron, with the energy of E', excites the second one, with the energy of E_0, to the

15) C. Mannenback, *Physica*, **17**, 1001 (1951); *ibid.*, **20**, 497 (1954).

conduction band and loses the minimum energy equal to the band gap energy, $\Delta\varepsilon$. In most organic crystals, the energy loss per collision is several eV for this process.

On the other hand, electron-phonon scattering involves a small energy loss per collision. Assuming that the phonon energy corresponds to the Debye temperature (for instance, it has been reported to be about 0.01 eV in naphthalene and anthracene.[16]), the average energy loss per collision at 300°K in organic crystals can be estimated to be about 0.003 eV. Note that it takes several hundred phonon-scattering events to produce as large an energy loss as one pair production event. Therefore, we consider pair-production scattering to be the main factor in the energy distribution of secondary electrons.

In their study of the energy distribution of photoelectrons from Cs_3Sb, Apker *et al.*[17] found evidence for the production of hole-electron pairs by energetic electrons. Spicer[18] determined the thresholds and the mean free path for pair production in semiconductors. Recently, pair-production scattering was investigated in detail by Spicer *et al.* for Cu and Ag[1] and by Kane for Si.[19]

In this work, we will consider only the escape probability of once scattered electrons in a way similar to that used for metal by Spicer *et al.*

Using a one-dimensional model, the total rate of the escape of electrons with energies between E and $E+dE$ after one scattering is*3:

$$N_S(E)dE \simeq AT(E)dE\int_{E+\varepsilon_{th}}^{h\nu-E_{th}} W(E')p(E,E')dE' \quad (11)$$

where $W(E')$ is the optical transition probability, where $p(E,E')$ is the probability that a primary electron with the energy of E' will be inelastically scattered to an energy between E and $E+dE$, where $T(E)$ is the surface transmission probability, where A is the function depending on the absorption coefficient and the scattering length, and where ε_{th} is the threshold energy for pair production.

Since we do not have enough information about the wavefunctions, particularly for excited states, the matrix element of electron-electron scattering is assumed to be constant. Under this approximation, and using the Fermi function at $T=0$, the following equation for $p(E,E')$ is obtained.[20]:

$$pdE = \frac{\rho(E)\left[\int \rho(E_0)\rho(E_0+E'-E)dE_0\right]dE}{\iint \rho(E)\rho(E_0)\rho(E_0+E'-E)dE_0dE} \quad (12)$$

Here, the scattering process by which an electron in the $(E,\vec{k'})$ state is scattered to the $(E,\vec{k})$ state and excites an electron in the $(E_0,\vec{k_0})$ state to the $(E_1,\vec{k_1})$ state is considered.

To ascertain the characteristic effects of a once-scatterd electron on the energy distribution, we assume a simple model. Assuming that $\rho(E)$, $\rho(E_0)$, and $\rho(E_0+E'-E)$ are constant, Eq. (12) reduces to:

$$pdE = dE\Big/\int_{-\Delta}^{E'-\varepsilon_{th}} dE = dE/(E'-\varepsilon_{th}+\Delta). \quad (13)$$

the lower limit of the integral means that we can neglect the interband transition for primary electrons. By substituting Eq. (13) into Eq. (11) and by assuming $AW(E')=W_0$ (const.) in Eq. (11), the following equation is derived:

$$N_s(E)dE \simeq W_0 dE T(E)\ln\frac{h\nu-E_{th}-\varepsilon_{th}+\Delta}{E+\Delta} \quad (14)$$

In Fig. 2 the energy distribution of secondary electrons, $N_s(E)$, is shown for several photon ener-

16) D. W. J. Cruickshank, *Rev. Mod. Phys.*, **30**, 163 (1958); M. L. Canut and J. L. Amaros, *J. Phys. Chem. Solids*, **21**, 146 (1961).

17) L. Apker, E. A. Taft and J. Dickey, *J. Opt. Soc. Amer.*, **43**, 78 (1953).

18) W. E. Spicer, *J. Phys. Chem. Solids*, **22**, 365 (1961).

19) E. O. Kane, *Phys. Rev.*, **159**, 624 (1967).

*3 Consider an electron excited to the energy of E' at a certain distance, x from the surface; the probability of this electron escaping with an energy between E and $E+dE$ after one scattering is the product of three probabilities: (1) the probability, p_1, that the primary electron will scatter after moving a certain distance, r, in the solids: (2) the probability, $p(E,E')$, that this electron will be scattered to an energy between E and $E+dE$, and (3) the probability, p_3, that it will escape without further scattering. Using a one-dimensional model, p_1 and p_3 are given as:

$$p_1 = \frac{1}{2}e^{-c'r}(c'dr),\quad p_3 = \frac{1}{2}T(E)e^{-c(x\pm r)},$$

where c' is the reciprocal scattering length for an electron with the energy of E' and where, generally, $c'>c$. The distance of the electron from the surface is $x-r$ $(0\leq r\leq x)$ and $x+r(0\leq r\leq\infty)$. The factor, 1/2, reflects the fact that the electron can go either towards the surface or away from it.

In an optical absorption process, the rate per unit of length at which electrons are excited to energies between E' and $E'+dE'$, in a slab with a width of dx located at a certain distance, x, from the surface, has the form:

$$G(E',x) = W(E')dE'e^{-\alpha x}dx.$$

By integrating the product of p_1, $p(E,E')$, p_3 and $G(E',x)$ over r and x under the assumption that the photoemissive crystal is semi-infinite, we obtain the following equation:

$$N_s(E',E)dEdE' = \left(\frac{2c'}{c'+c}-\frac{\alpha+c}{\alpha+c'}\right) \times \frac{c'}{4(c'-c)(\alpha+c)}T(E)W(E')p(E,E')dEdE'.$$

By setting $A = \left(\frac{2c'}{c'+c}-\frac{\alpha+c}{\alpha+c'}\right) \times \frac{c'}{4(c'-c)(\alpha+c)}$ in the above equation, we obtain Eq. (11).

20) Ref. 1, p. A1035; Peierls, Quantum theory of solids (Oxford, 1955) p. 131.

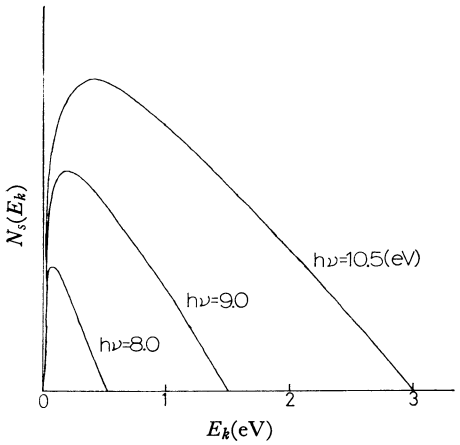

Fig. 2. Theoretical energy distribution of once-scattered electrons.

gies, setting $T(E) \propto E^{1/2}$, $E_{th}=5.5$ eV, $\varepsilon_{th}=2.0$ eV, and $\Delta \simeq 0$ in Eq. (14).

The most important feature of Fig. 2 is that pair-production scattering gives a low energy peak in the energy distribution of photoemitted electrons. The position of the peak remains almost constant in energy above the vacuum level and the height of the peak increases, as the photon energy increases. These results are in qualitative agreement with the results obtained for metal by Spicer:[1] Spicer used a three-dimensional model and introduced the "threshold function" in place of $T(E)$. Though the choice of Δ(defined in Fig. 1) has a slight influence on the curvature and the position of the peak, its behaviour described above does not change.

Experimental

The details of the purification of samples and the arrangement of the specimens in the photoemission measurement have been reported previously.[9,10],*4

2.1. Sample. Figure 3 shows the materials—anthracene, naphthacene, pentacene, perylene, quaterrylene, tetrathionaphthacene, and indanthrone—used in the present work. All the purified samples except anthracene were deposited on a copper disk, 10 mm in diameter, by means of a sublimation method *in vacuo* (10^{-6} Torr), the thickness of the film being a few microns. The single crystal of zone-refined anthracene[21] was attached to the copper disk by silver paste, its thickness being about 100 μ.

2.2. Experimental Technique. The photoemission was measured with a 0.5-metre Seya-Namioka-type vacuum ultraviolet monochromator. A concave grating coated by MgF_2, with 1200 grooves /mm, has a reciprocal linear dispersion at the exit slit of 16 Å/mm. A lithium fluoride window, which was attached with an O-ring to the exit slit, transmitted to a photon energy of about 11.5 eV. As a light source, a Hinteregger-type hydrogen discharge lamp was used. A collector was a glass sphere about 13 cm in diameter; on the inside it was coated with a conducting layer of colloidal graphite, Aguadag. An organic compound deposited onto a copper disk was fixed at the centre of the collector. Light was focussed on the sample in a spot with dimensions of about 6 mm×6 mm.

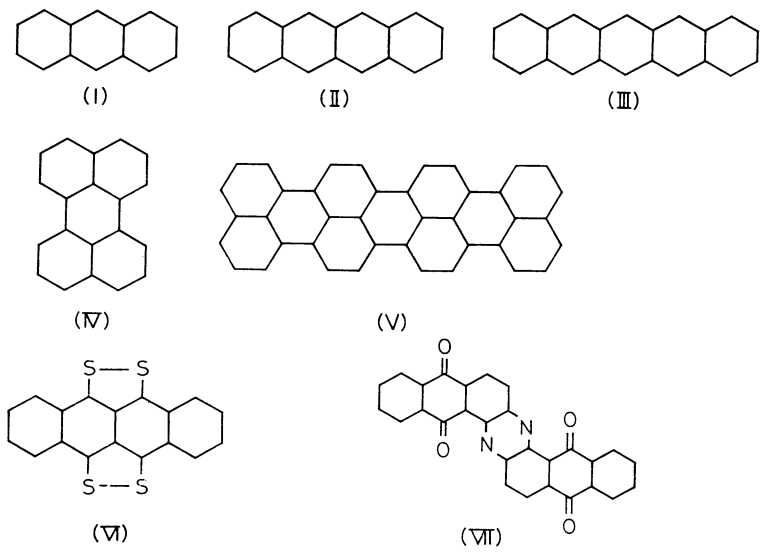

Fig. 3. Structural formula of materials.
(I) anthracene, (II) naphthacene, (III) pentacene, (IV) perylene, (V) quaterrylene, (VI) tetrathionaphthacene, and (VII) indanthrone.

*4 The method of purifying quaterrylene was reported by Y. Maruyama, H. Inokuchi and Y. Harada, This Bulletin, **36**, 1193 (1963).

21) S. Iwashima, K. Ogino and J. Aoki, *Nippon Kagaku Zasshi*, **89**, 338 (1968).

The photoemission current was amplified and observed by a Cary 31 vibrating-reed electrometer. Its spectral response was measured at intervals of 20 Å under an applied potential of 10 V, high enough to collect all the photoemitted electrons.[22]
One-mm slits were used in these experiments. The 16 Å/mm reciprocal dispersion at the exit slit gives, then, a photon-energy spread of 0.05 eV at 6.20 eV (2000 Å) and one of 0.13 eV at 10.33 eV (1200 Å).

The quantum yield, Y, was found from the ratio between the number of the photoemitted electrons and that of the incident photons. The absolute measurement of the incident photons was made by means of an Epply circular thermopile. The relative value of the light intensity was obtained by measuring the fluorescence intensity from a coronene film[23] evaporated onto a glass plate with a RCA 5819 photomultiplier tube.

The energy distribution curves (EDC) were obtained by differentiating graphically the current-voltage characteristics, which had been measured by the spherical retarding-potential method and recorded with a Yokogawa X-Y recorder, PRO-12. The estimated uncertainty in the location of structures in EDC was ±0.2 eV.

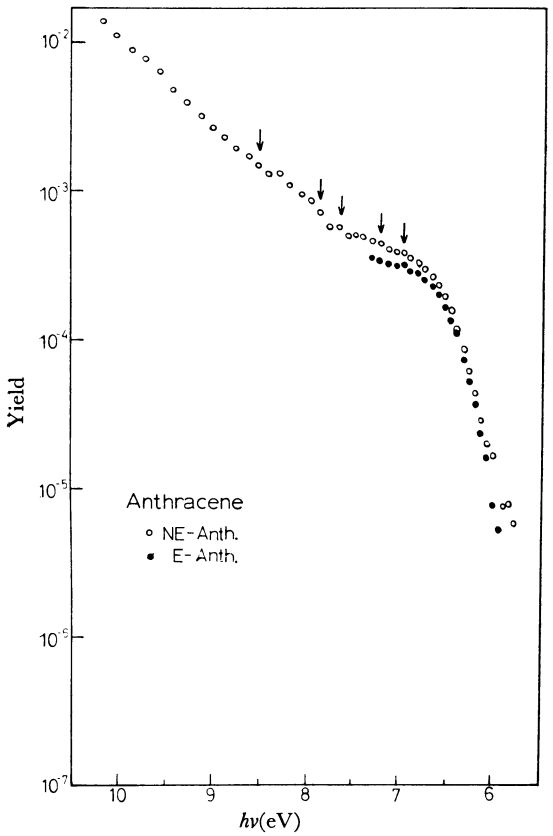

Fig. 4. Spectral distribution of the quantum yield for anthracene.

22) T. Hirooka, M, Kochi, H. Inokuchi, Y.Harada and J. Aihara, This Bulletin **42**, 1481 (1969).
23) H. Inokuchi, Y. Harada and T. Kondow, *J. Opt. Soc. Amer.*, **54**, 842 (1964).

Results

3.1. Quantum Yield. Figure 4 shows the spectral distributions of the quantum yield for anthracene single crystal on the *a-b* plane under illumination. This single crystal was measured under a pressure of 10^{-3} Torr, because it evaporated easily in a high vacuum. One distribution was observed as soon as the photo-cell had been evacuated to a pressure of 10^{-3} Torr (this will be referred to as not-evaporated-anthracene, NE-Anth.). The other distribution was observed after more than five hours evacuation*5 (this will be referred to as evaporated-anthracene, *E*-Anth.). The most conspicuous difference between the two cases was that a tail appeared for NE-Anth. in the photon-energy region lower than 5.9 eV. This seems to indicate that NE-Anth. has two kinds of ionization potential, the larger value corresponding to that of anthracene itself, and the smaller one, to that of the impurity formed on the surface layer of the anthracene crystal. We will again discuss this problem in Section 4.4. The other features of the spectra were not so different in the two cases, though the magnitude of the yield for NE-Anth.

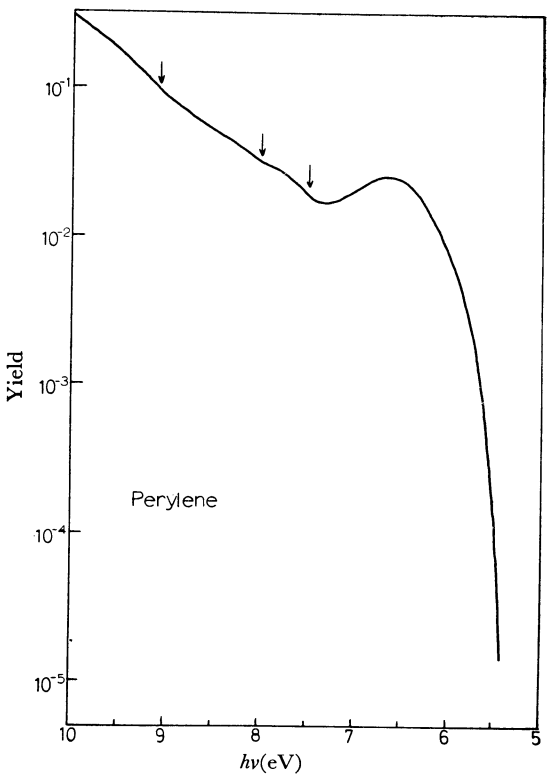

Fig. 5. Spectral distribution of the quantum yield for perylene.

*5 There was hardly any influence of evacuation when the photo-cell was evacuated for more than two hours.

was slightly higher than that for *E*-Anth.

Figure 5 shows the spectral response of the quantum yield for perylene. As can be seen in Fig. 5, a decrease in the yield was observed at photon energies between 6.8 and 7.3 eV. In Section 4.2, using the data of the energy distribution, it will be found that this decrease can be interpreted as the effect of pair-production scattering.

As may be seen from Figs. 4 and 5, the quantum yield of organic crystals rose with a considerable sharpness at the threshold and increased quickly with an increase in the photon energy. In the higher-energy region, the value of the yield increased gradually, reaching the order of 10^{-2}—10^{-1} electrons/photon at a photon energy of about 10 eV. Further, some inflection points were observed in the region more than 1 eV above the threshold.

3.2. Energy-distribution Curve and Energy-loss Curve. Figures 6, 7, and 8 show the energy distribution curves (EDC) for anthracene,*[6] perylene, and quaterrylene respectively, normalized

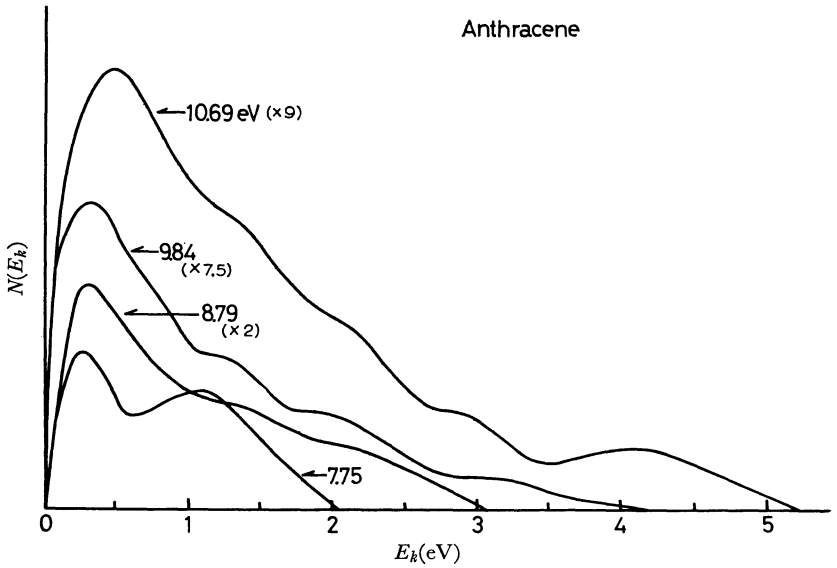

Fig. 6. Energy distribution curve for anthracene.

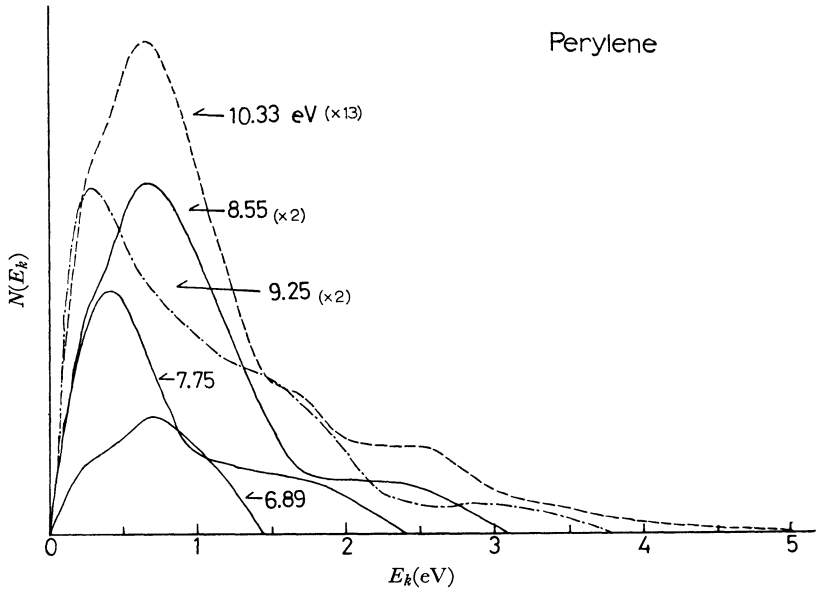

Fig. 7. Energy distribution curve for perylene.

*[6] A very slight increase in the current was observed above the saturation point in the current-voltage characteristics of the anthracene single crystal. Therefore, in the EDC for anthracene the tails due to an unsaturated current were cut off at the saturation voltage.

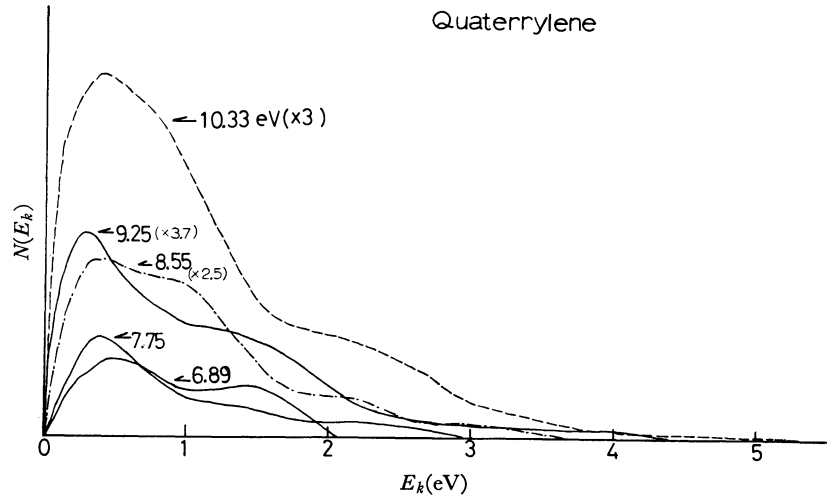

Fig. 8. Energy distribution curve for quaterrylene.

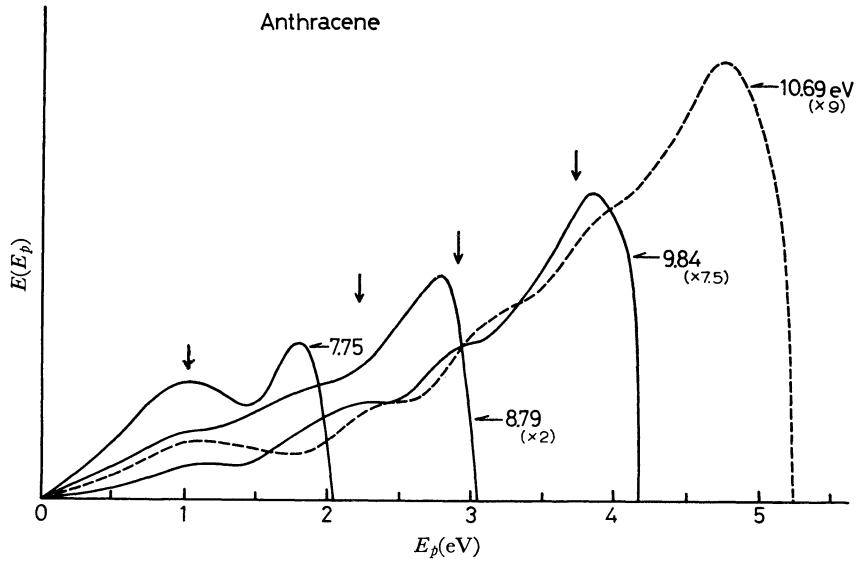

Fig. 9. Energy-loss curve for anthracene.

to the yield. On the ordinate axis, the relative numbers of the emitted electrons, $N(E)$, are plotted; on the abscissa axis, the electron energies, E_k, are stated relative to the vacuum level.

In Figs. 9, 10, and 11 the energy-loss curves (ELC) are shown; in them the difference, E_p, ($E_p = E_m - E_k$, E_m is the maximum kinetic energy) has been chosen on the abscissa axis instead of the electron kinetic energy, E_k. In this representation the $E_p=0$ point corresponds to electrons with a limiting maximum kinetic energy at any photon energy. The numerical values, increasing to the right, represent a deficiency in kinetic-energy losses.

As can be seen from EDC (Figs. 6, 7, and 8), two groups of photoelectrons were observed. The one formed by slow electrons was almost stationary in the same kinetic energy range (0.3—0.5 eV), independent of the increase in photon energy, while the height of their peaks increased as the photon energy increased. The group of fast electrons was regularly shifted to kinetic energies higher by the same amount as the photon energy increased.

The behaviour of the fast electrons can be described more pertinently in ELC. For the anthracene single crystal (see Fig. 9), at the photon energy of 7.75 eV ELC had a maximum at $E_p \simeq$ 1.0 eV. When the photon energy was increased to 8.79 eV, a shoulder appeared at $E_p \simeq 2.0$ eV. Subsequent shoulders appeared at $E_p \simeq 2.9$ and 3.7 eV at higher photon energies. The positions of the maxima and shoulders were independent

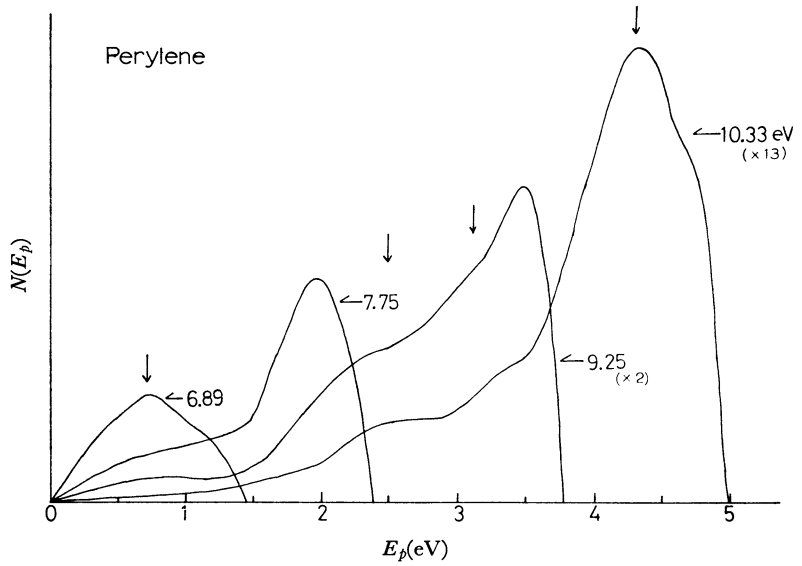

Fig. 10. Energy-loss curve for perylene.

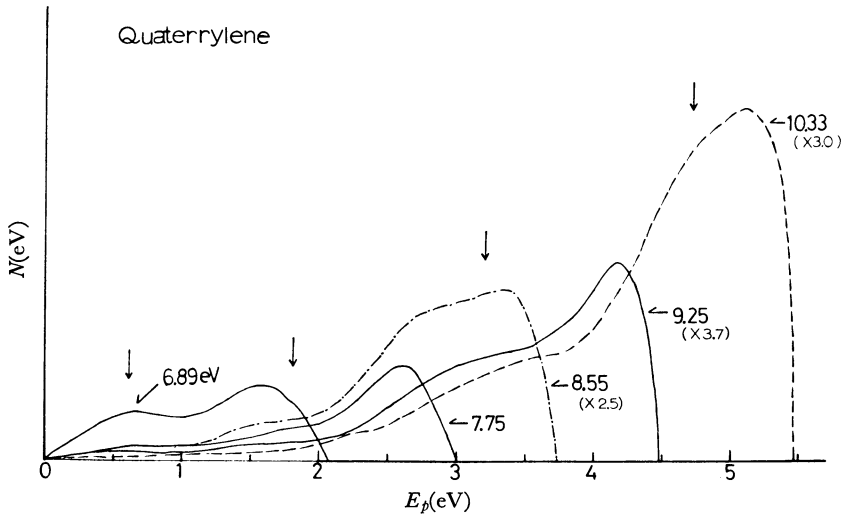

Fig. 11. Energy-loss curve for quaterrylene.

of the photon energy. The ELC of other compounds were qualitatively similar to that of anthracene.

For photon energies at which inelastic scatterings were not so frequent, broad energy-loss distributions due to vibrational excitation were clearly observed, with the maxima between $E_p=0.6$ eV and 1.0 eV (see Figs. 9, 10, and 11). Those distributions increased almost linearly with the increase in the energy-loss, commencing at $E_p=0$.

Discussion

4.1. Application of the Model to Organic Crystals. The quantum yield near the photoelectric threshold for all compounds was plotted on various power-law assumptions in order to establish the spectral characteristics. A typical example of such data is shown in Fig. 12, where the yield for the anthracene single crystal is plotted to the 1,1/2, and 1/3 power versus $h\nu$. These results, and those for other samples, indicate that the cubic power most closely represents the data and that the yield in this region obeys the relations:

$$Y \propto (h\nu - E_{th}^*)^3 \qquad (15)$$

where E_{th}^* is defined as the extraporated threshold value of the cube-root plots, such as are shown in the insets of Fig. 13. This empirical cube-law is in good agreement with the power-law predicted by Eq. (10), which may be considered to show that the form of the yield near the thresh-

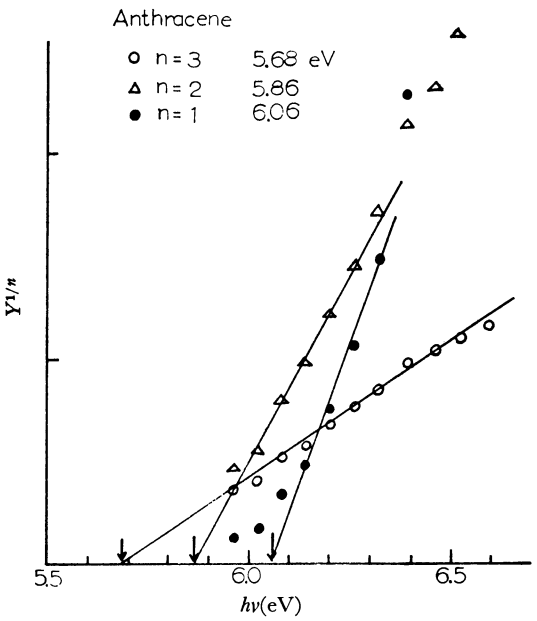

Fig. 12. Power-law fit for the photoelectric yield near the threshold for anthracene.

old for organic crystals can be effectively determined by the vibrational transition probability $|<n|0>|^2$ and the surface transmission probability $T(E)$. The importance of the $|<n|0>|^2$ factor in the photoemission of organic crystals and its linearity for n were implied by Williams and Dresner.[24]

The semi-empirical cube-power law expressed by Eq. (10) has certain limits for its validity, limits which come from the form of $T(E)$ assumed by Eq. (9). However, it is theoretically known that the $T(E)\propto E^{1/2}$ relation corresponds to the case of a rectangular potential wall.[25] Apker *et al.* used the $T(E)\propto E$ form in their analysis of the energy and spectral distribution of semiconductors.[26] Regarding the (b) assumption of our model, localized states are generally expected to exist in the continuum in molecular crystals. Although its influence was not observed in the present work, it is an important subject deserving future attention.

Figure 13 shows a cube-root-plot for each compound. In Table 1 the threshold values, E_{th}* and E_{th}, are listed and compared with those obtained by other workers. E_{th} was determined by extrapolation to a quantum yield of 10^{-7} electrons per incident photon. As can be seen from Table 1, the E_{th}* values show reasonable agreement with the E_{th} values and those of other workers.

In addition, the cube-law had been applied to determine the photoelectric threshold energy of charge-transfer complexes.[22] For those complexes the quantum yield near the threshold dropped so slowly that the threshold energy could not be determined by the extrapolation method.

4.2. Pair-production Scattering. As can be seen from EDC for perylene (Fig. 7), a remarkable low-energy peak appeared at $h\nu=7.75$ eV. Since an electron with the energy of E, less than ε_{th}, cannot escape after pair-production scattering, a low-energy peak due to pair production begins to appear in EDC at the photon energy of $h\nu\geq E_{th}+\varepsilon_{th}$. Note that perylene has a threshold energy of $E_{th}\simeq 5.40$ eV and a bandgap energy of $\Delta\varepsilon=1.95$—2.2 eV.[27] At photon energies of more than 7.75 eV, the low-energy peak was almost stationary at $E_k\simeq 0.5$ eV and grew rapidly in relative height with the increase in photon energy. Further, it was found that relatively few electrons escaped into a vacuum with kinetic energies larger than about 2 eV (see Fig. 7). These phenomena are expected from theoretical considerations for pair production (see Fig. 2). Now, we can attribute the behaviour of the low-energy peak and the scarcity of electrons with higher kinetic energies to pair-production scattering.

On the other hand, the decrease in the quantum yield is expected to occur in the $h\nu\leq E_{th}+\varepsilon_{th}$ region of the photon energy if the inelastic scattering takes place efficiently. The pair-production process is a kind of multiple process, and a decrease in quantum yield due to this process was observed in the photoemission of alkali halides.[28] For perylene, the decrease in the yield was observed in the $h\nu=6.8$—7.3 eV region (see Fig. 5). Therefore, we estimate that the threshold for the pair production of perylene is nearly equal to its band-gap energy.

For quaterrylene there are few electrons with energies larger than about 2 eV (see Fig. 8). Further, a decrease in the yield for quaterrylene had been observed between 2.2 and 2.7 eV above the photoelectric threshold by Harada.[29] The band-gap energy of quaterrylene has been reported to be 1.7 eV or more.[30] Therefore, the threshold for pair production is estimated to be a little more than its band gap.

24) R. Williams and J. Dresner, *J. Chem. Phys.*, **46**, 2133 (1967).
25) L. D. Landau and E. M. Lifshitz, "Quantum Mechanics, Nonrelativistic Theory," Pergamon Press, New York (1965), p. 77.
26) L. Apker, E. Taft and J. Dickey, *Phys. Rev.*, **74**, 1462 (1948).
27) M. Sano and H. Akamatu, This Bulletin, **34**, 1569 (1961); D. C. Northrop and O. Simpson, *Proc. Roy. Soc.*, **A234**, 124 (1956).
28) P. H. Metzger, *J. Phys. Chem. Solids*, **26**, 1879 (1965).
29) Y. Harada, The thesis for the degree of doctor (Tokyo University).
30) Y. Maruyama and H. Inokuchi, This Bulletin, **39**, 1418 (1966).

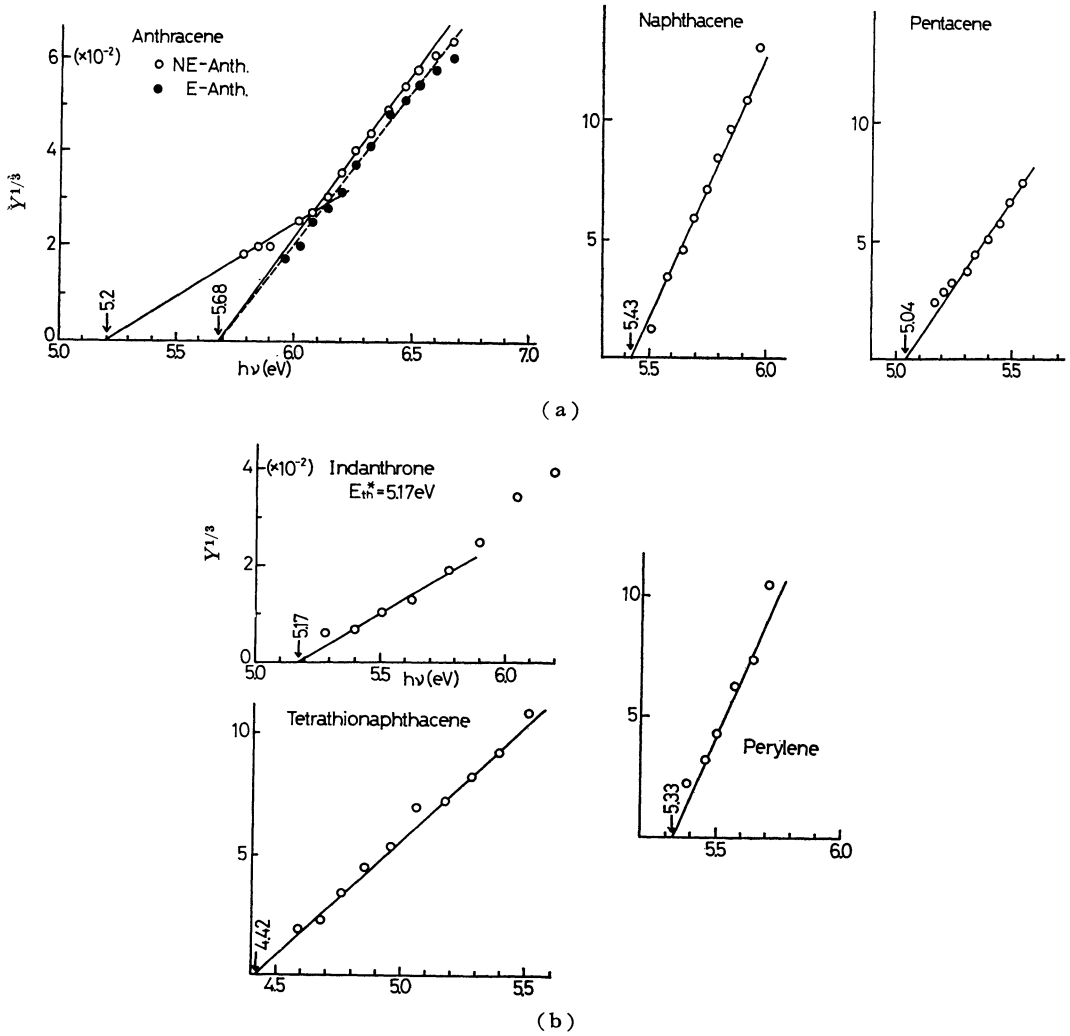

Fig. 13. Cube power-law fit for the photoelectric yield near the threshold.

TABLE 1. PHOTOELECTRIC THRESHOLD AND IONIZATION POTENTIAL FOR THE ORGANIC CRYSTALS (in eV)

Compound	E_{th}	E^*_{th} $(=I_c)$	Other Work	I_G
Anthracene	5.65	5.68 (5.2)	5.65[a], 5.0—5.6[b]	7.38[b]
Naphthacene	5.40	5.43	5.24[c], 5.25[b], 5.31[d]	6.88[b]
Pentacene	5.06	5.04	5.06[c], 5.1[b]	
Perylene	5.40	5.33	5.40[d]	7.22[f], 7.06[g]
Indanthrone	5.10	5.17		
Tetrathionaphthacene	4.55	4.42	4.56[c], 4.45—4.54[e],*	

a) Ref. 5, b) Ref. 31, c) Ref. 9, d) Ref. 37, e) Ref. 34, f) Ref. 38, g) Ref. 39.
* This value was obtained using the observed values for work function and band gap energy (see H. Inokuchi, M. Kochi, Y. Harada, This Bulletin, **40**, 2695 (1967)).

37) M. Batley and L. E. Lyons, *Mol. Cryst.*, **3**, 357 (1968).
38) J. Briegleb, "Electronen-Donator-Acceptor-Komplexes," Springer-Verlag, Berlin (1961).
39) M.Kinoshita, This Bulletin, **35**, 1609 (1962).

For the anthracene single crystal, the threshold for pair production could not be estimated because the scarcity of energetic electrons in EDC and the decrease of the yield were not remarkable. It may be due to the inelastic scattering on the crystal surface.

4.3. Energy Structures of Organic Crystals. In ELC for anthracene (Fig. 9) the position of the first maximum was located at $E_p \simeq 1.0$ eV; the second shoulder, at $E_p \simeq 2.2$ eV; the third, at 2.9 eV, and the fourth at 3.7 eV, independent of the photon energy, meaning losses of 1.2, 1.9, and 2.7 eV respectively relative to the position of the first maximum. These results are in good agreement with that of Vilessov and Terenin.[31]

We reported[10] previously that the structures of this kind observed in ELC should be ascribed to those of valence bands. The structures which do not shift in ELC and which do shift in EDC linearly with the photon energy can be explained in terms of the so-called nondirect transition.[1,2] Schechtman and Spicer[32] found that these structures were observed very clearly for phthalocyanines under a high vacuum of 10^{-9} Torr.

At energies near the threshold for transitions from deeper bands, the yield may be expected to rise as a result of the larger density of possible initial states. In Figs. 4 and 5 the inflection points are illustrated by arrows. For anthracene they were situated at 6.93, 7.18, 7.61, 7.83, and 8.48 eV, thus meaning energies higher by 1.28, 1.53, 1.96, 2.18, and 2.83 eV respectively relative to the threshold energy, $E_{th} \simeq 5.65$ eV.

In Table 2, the discrete energy losses and the inflection points are given relative to the position of the first maximum and to the threshold value, respectively.*[7] In the table of anthracene, the two sets of values marked by (*) may show the lifting-up of the accidental degeneracies of the π-orbital energy, which are annexed to the LCAO method.[33] As may be seen from Table 2, the sequence of the descrete energy losses is well reproduced in the sequence of the inflection points in the yield, taking into consideration the resolution of ELC. This means that the discrete energy losses in ELC and the occurrence of inflection points in the yield spectra can be accounted for by assuming the existence of additional valence bands. It should also be noted that the fairly broad width of the first peak in ELC is due to the vibrational structure of the valence band. In order to ensure our observed valence band structure, a reliable method for the calculation for organic molecules is under consideration.

Table 2. Energy structure of the valence band (in eV)

Anthracene

Y		ΔY	E_p	ΔE_p
5.65		0	1.0	0
6.93 7.18	(*)	1.28 1.53	2.2	1.2
7.61 7.83	(*)	1.96 2.18	2.9	1.9
8.48		2.83	3.7	2.7

Perylene

Y	ΔY	E_p	ΔE_p
5.40	0	0.7	0
7.53	2.13	2.5	1.8
8.00	2.60	3.1	2.4
9.05	3.65	4.3	3.6

Quaterrylene

Y*	ΔY	E_p	ΔE_p
4.76	0	0.6	0
—	—	1.8	1.2
7.6	2.8	3.2	2.6
8.5	3.7	4.7	4.1

* Ref. 29.

4.4. Photoelectric Threshold Energy of Organic Crystals. The energy required to extract an electron from an organic crystal to a point in a vacuum outside its surface, *i.e.*, the photoelctric threshold energy, was obtained by measuring the quantum yield. The threshold energy, E_{th}*, corresponds to the ionization potential, I_C, of the crystal.

Table 1 summarizes the data for the threshold energies for the different organic crystal compounds studied in the present work. The table also includes data obtained by other workers and those for molecular ionization potentials, I_G. The values for I_C were obtained by extrapolation to $Y=0$ using the power-law of $Y \propto (h\nu - E_{th}^*)^3$. Regarding the column of "Other Work", Terenin and Vilessov[31] obtained their values from the measurement of the maximum kinetic energy. Kotani and Akamatu[34] determined the work function of organic crystals using a contact potential-difference method.

The table shows that the I_C values of the organic crystals under consideration are below I_G by 1—

31) A. Terenin and F. Vilessov, "Advances in Photochemistry," Vol. 2, Interscience Publ., New York (1964), p. 385.

32) B. H. Schechtman and W. E. Spicer, *Chem. Phys. Lett.*, **2**, 207 (1968).

*7 When ELC are measured with sufficient accuracy in the future, the rising points in ELC should be compared with the inflection points in the yield spectra.

33) C. A. Coulson, *J. Phys. Soc.*, **60**, 257 (1948).

34) M. Kotani and H. Akamatu, private communication.

2 eV. As has been suggested by Lyons,[35] this difference may be due to the polarization energy of the crystal by a positive centre.

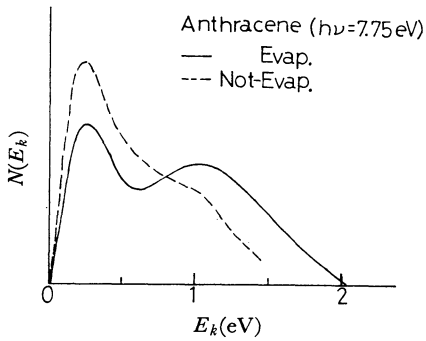

Fig. 14. Effect of oxygen on EDC for anthracene single crystal.

35) L. E. Lyons, *J. Chem. Soc.*, **1957**, 5001; L. E. Lyons and J. C. Mackie, *Proc. Chem. Soc.*, **1962**, 71.

For the I_C of the anthracene single crystal, we obtained two values for NE–Anth. One was 5.68 eV, which agreed with the I_C of E–Anth.; the other was about 5.2 eV. As Pope and Burgos[36] pointed out, the lower value for I_C seems to be caused by the oxygen-anthracene pair formed on the surface of the anthracene crystal. Figure 14 shows the energy distribution curves at $h\nu=$ 7.75 eV for both E–Anth. and NE–Anth. It can be seen from the figure that the number of slow electrons for NE–Anth. is larger than that for E–Anth.; this may be attributed to an inelastic collision on the crystal surface between photoelectrons and the oxygen-anthracene pair.

The authors gratefully acknowledge their valuable discussions with Professor Yutaka Toyozawa, The University of Tokyo.

36) M. Pope and J. Burgos, *Mol. Cryst.*, **1**, 395 (1966).